A&A 565, A92 (2014)
DOI: 10.1051/0004-6361/201323327

Astronomy & Astrophysics

Spectro-astrometry of V1515 Cygni⋆,⋆⋆ *(Research Note)*

V. Agra-Amboage[1] and P. J. V. Garcia[1]

Universidade do Porto, Faculdade de Engenharia, Departamento Engenharia Fisica, SIM Unidade FCT nº4006, rua Dr. Roberto Frias, s/n 4200-465 Porto, Portugal
e-mail: vaa@fe.up.pt; pgarcia@fe.up.pt

Received 23 December 2013 / Accepted 24 March 2014

ABSTRACT

Context. FU Orionis objects are a class of young stars with powerful bursts in luminosity that show evidence of accretion and ejection activity. It is generally accepted that they are surrounded by a Keplerian circumstellar disk and an infalling envelope. The outburst occurs because of a sudden increase in the accretion rate.
Aims. We study the regions closer to the central star in order to observe the signs of the accretion and ejection activity.
Methods. We present optical observations of the H_α line using the Integral Field Spectrograph OASIS, at the *William Herschel* Telescope, combined with adaptive optics. Since this technique gives the spectral information for both spatial directions, we carried out a two-dimensional spectro-astrometric study of the signal.
Results. We measured a clear spectro-astrometric signal in the north-south direction. The cross-correlation between the spectra showed a spatial distribution in velocity suggestive of scattering by a disk surrounding the star. This would be one of the few spatial inferences of a disk observed in an FU Orionis object. However, to fully understand the observed structure, higher angular and spectral resolution observations are required. V1515 Cyg now appears to be an important object to be observed with a new generation of instruments to increase our knowledge about the disk and outflow structure in FU Orionis objects.

Key words. techniques: imaging spectroscopy – stars: pre-main sequence – stars: individual: V1515 Cyg – stars: winds, outflows – protoplanetary disks

1. Introduction

FU Orionis objects (FUor) are a class of young stellar objects showing powerful outbursts, increasing in luminosity about five magnitudes and changing their spectral type on short timescales. The typical rise time is over one year, whereas the timescale for the lifetime of the high phase is decades. Two main theories have been proposed to explain their nature. The first one favors a scenario where an unstable star is rotating near breakup, which would cause the outburst. A rapidly rotating G supergiant photosphere enveloped by a rising cooler shell could explain the observed spectral properties of these objects (Herbig et al. 2003). The second model, which is more widely accepted nowadays, considers a protostellar object surrounded by a Keplerian circumstellar disk and an infalling envelope. The outburst would occur because of a sudden increase in the accretion rate through the disk. In this scenario, all young stars experience FUor phases during their evolution (Hartmann & Kenyon 1985, 1996). Many studies during the past years investigated the accretion phenomenon in this class of objects from both an observational and a theoretical point of view. Despite all this effort, the origin of the episodic accretion and outburst is poorly understood. A detailed review by Audard et al. (2014) includes promising directions.

Evidence of outflows in FUor objects have already been reported before by different authors using different observational tracers, both in the optical and in the infrared (IR; Croswell et al. 1987), and showing P Cygni profile in different lines, such as several hydrogen lines, lower excitation lines of neutral metals and TiO bands (Hartmann & Kenyon 1996), and continuum radio observations (Rodríguez & Hartmann 1992). For the Z CMa system in particular (Herbig Be star and FUor object), Whelan et al. (2010) detect jets driven by each of the components in the [FeII] lines. At much smaller scales, Benisty et al. (2010) detect collimated Brγ from the Be component. Typical observed wind velocities are in the range of 300–400 km s^{-1} with mass-loss rates of $\sim 10^{-5}$–10^{-6} $M_\odot$ yr^{-1}, even if this is a very variable parameter from one source to another. In the case of V1515 Cyg, discovered by Herbig (1977), evidence of winds and outflows have been found. Both Bastian & Mundt (1985) and Croswell et al. (1987) showed spectra with a clear H_α P Cygni profile, and Croswell et al. (1987) determined a mass loss rate of 10^{-5} $M_\odot$/yr from the spectral energy distribution (SED). This value was then confirmed by Kenyon et al. (1991). They compared the mid- and far-infrared SED to the predictions of standard accretion disk models and concluded that the presence of an infalling envelope in this object is needed to fit the model, but the presence of a cavity in the envelope, through which the central optical source is seen, is also required. More recently, Green et al. (2006) have reached similar conclusions. Using IR *Spitzer*/IRS observations, they also conclude that the envelope model requires an outflow hole with a large opening angle. They suggest that this cavity should be the result of the high mass-loss rate accompanying rapid accretion in the FUor outburst state.

Despite the evidence of winds/outflows and accretion activity in these objects, a detailed study of their physical properties has been difficult to carry out with high-resolution instruments manly due to the faintness of these objects and their distance

⋆ Based on service observations made with the WHT operated on the island of La Palma by the Isaac Newton Group in the Spanish Observatorio del Roque de los Muchachos of the Instituto de Astrofísica de Canarias.

⋆⋆ All the figures are available in color in electronic form.

Table 1. Summary of observations taken on 3 September 2005.

Object	Configuration	UT	T_{exp} (s)	Airmass
V1515 Cyg	HR638	01:30	1800	1.28
V1515 Cyg	HR638	02:01	1800	1.39
Neon Lamp	HR638	02:34	12	
Standard star (G191-B2B)	HR638	04:51	1500	1.23
Neon Lamp	HR638	04:48	12	
V1515 Cyg	HR667	00:24	1800	1.12
V1515 Cyg	HR667	00:55	1800	1.18
Neon Lamp	HR667	01:26	3	
Standard star (G191-B2B)	HR667	05:17	1500	1.18
Neon Lamp	HR667	05:43	12	

Notes. The configuration HR667 was used to observe the H_α line and HR638 for the [OI], both configurations with a sampling of 0.″26.

to us; for instance, V1515 Cyg is 1 kpc away (Racine 1968). Here, we present a new approach through an integral field spectroscopy study at medium spatial resolution, which allows us to astrometrically probe scales typically in the range of 100–1000 AU to the central star and carry out a spectroscopic study in both spatial directions simultaneously.

This article is organized as follows. In Sect. 2 we describe the observations and the data reduction, and in Sect. 3 we present our results in terms of detection and reality of the detection. Section 4 proposes some explanations for the observed signal in the context of the previous works and summarizes our conclusions.

2. Observations and data reduction

Observations of V1515 Cyg were obtained at the *William Herschel* Telescope with the Integral Field Spectrograph OASIS combined with the adaptive optic module NAOMI mounted at the Nasmyth focus. The summary of the observing run is presented in Table 1. Two different configurations were used, HR638 to observe the [OI] line and HR667 for the H_α line, with a final spatial sampling of 0.″19, which gives a field of view (FOV) of 9.″5 × 7.″2. The first configuration, HR638, provides a spectral resolution of 3190 in a wavelength range between 6210 Å and 6550 Å, sampled at 0.96 Å/px. The second configuration, HR667, provides a spectral resolution of 3340 for a wavelength range of 6490–6840 Å, sampled at 0.97 Å/px. For each configuration, two exposures of 1800s each were taken. After adaptive optic correction, the effective spatial resolution achieved is 0.″7 (Gaussian core FWHM).

Data was reduced using the XOasis software provided by the OASIS team in Lyon (France)[1]. The raw images are bias-subtracted. To extract the spectra, the positions of the microlenses on the CCD were obtained by a micro-pupil image taken during the observation run. This image is obtained by illuminating the instrument with a source of uniform light with the dispersive element removed. In this image a Gaussian fit is carried out to obtain the center of each micro-pupil. Then, a cross-dispersion profile is evaluated for each spectrum and then fitted using an algorithm that computes an optical model of the instrument dispersion on the detector. The positions of the spectra ridges are obtained from these cross-dispersion profiles. For each lens and each wavelength, the CCD pixels are summed up over a total width of five pixels centered on the positions determined before. Each summed pixel has a weight that is computed with an optimal algorithm (Horne 1986), using the photon noise of the fraction of the signal on the pixel and the known CCD readout noise. Finally an extraction mask is created and the extracted spectra are arranged in a data cube with the two spatial dimensions and a first estimation of the wavelength vector.

Using a neon lamp, a refined wavelength calibration is carried out by fitting the residuals of the first estimation, made in the previous step, to a second-order polynomial. The low-frequency spatial and spectral flat effects are corrected in the same step using a sky flat and the continuum frames (images where the instrument is illuminated with uniform light). Then, the data cube is corrected from cosmic rays. The correction makes use of the spectral similarity between each spectrum and those in its neighboring region, usually twice the size of the spatial sampling. The integrated fluxes of the spectrum and of the neighbors are computed. The neighbors' spectra are normalized to the central one, and the median of the spectra is calculated. The difference between the central spectrum and the median spectrum is computed (median-filtered difference) and compared with the unfiltered difference. A sigma-clipping is then performed on the resulting spectrum. The pixels above 30 times sigma are replaced in the central spectrum by the median value. The flux calibration is carried out using the standard star image, over which all the previous steps are also carried out. Finally, the data cubes are resampled to a square spatial sampling grid.

3. Results

3.1. Spectro-astrometry

The spectro-astrometry technique measures the astrometric position by a Gaussian fit of the spatial profiles for each individual wavelength (e.g., Whelan & Garcia 2008). In the case of integral field spectroscopy, where the spectral information is given for each 2D spatial point, this technique can be applied to both spatial directions (see as example Davies et al. 2010). Here, a 2D circular Gaussian is fitted to each image of the data cube, with a Levenberg-Marquardt algorithm. The wavelength-dependent Gaussian centers and Gaussian full width at half maximum (FWHM) are the spectro-astrometric signal. Only the differential signals are presented and a linear contribution was removed by fitting a straight line to the data. Figures 1 and 2 show, for each individual exposure, the detected spectro-astrometric signal in the spatial directions for the spectral region around the H_α6562 Å line. Top panels show the horizontal direction on the detector, oriented west-east (positive ΔX is east), the middle ones refer to the vertical direction, oriented from south to north, and the bottom panels show the differential FWHM from the fit. The profile of the emission, arbitrarily normalized in order to include it in the plot, is also plotted in blue. The wavelength scale is converted to a radial velocity scale taking the vacuum wavelength of H_α as the reference velocity and a heliocentric correction for V1515 Cyg of -12 ± 2 km s^{-1} (Herbig 1977).

The P Cygni profile previously observed in this object (Bastian & Mundt 1985) is clear in our data, too. A small spectro-astrometric signal is detected in the horizontal direction. However, considering the error bars, the signal in the vertical direction is clearly detected at blueshifted velocities of ∼−100 km s^{-1}. The FWHM increases in the absorption part of the PCygni profile, for the same velocities. The differential

[1] http://www.cfht.hawaii.edu/Instruments/Spectroscopy/OASIS/Reduc/

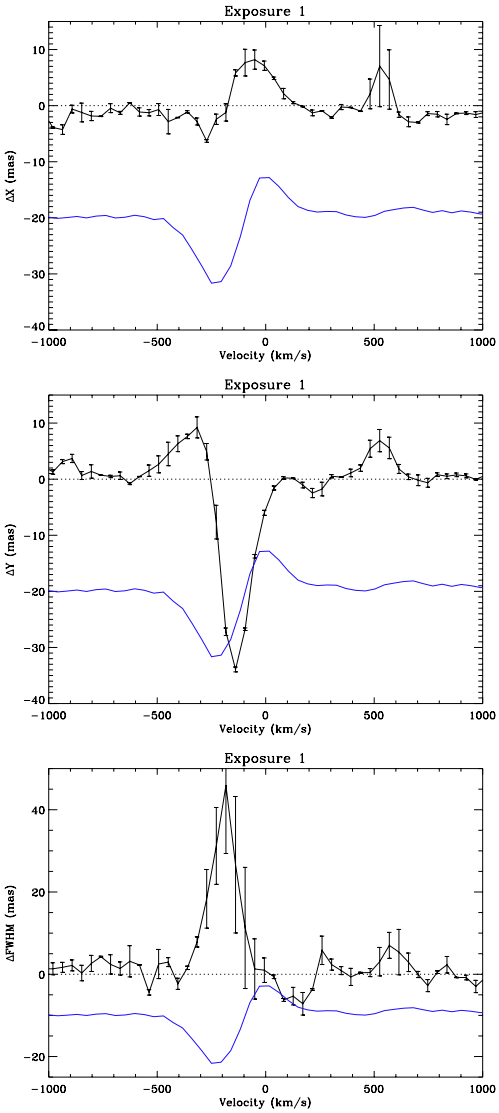

Fig. 1. For the first individual exposure, Gaussian centers of the spectro-astrometric signal as a function of the velocity in both the W-E (east for $\Delta X > 0$) and S-N (north for $\Delta Y > 0$) directions, in top and middle panels, respectively. Bottom panel shows the differential FWHM, see text. The H_α line profile is overplotted in blue showing a clear P Cygni profile.

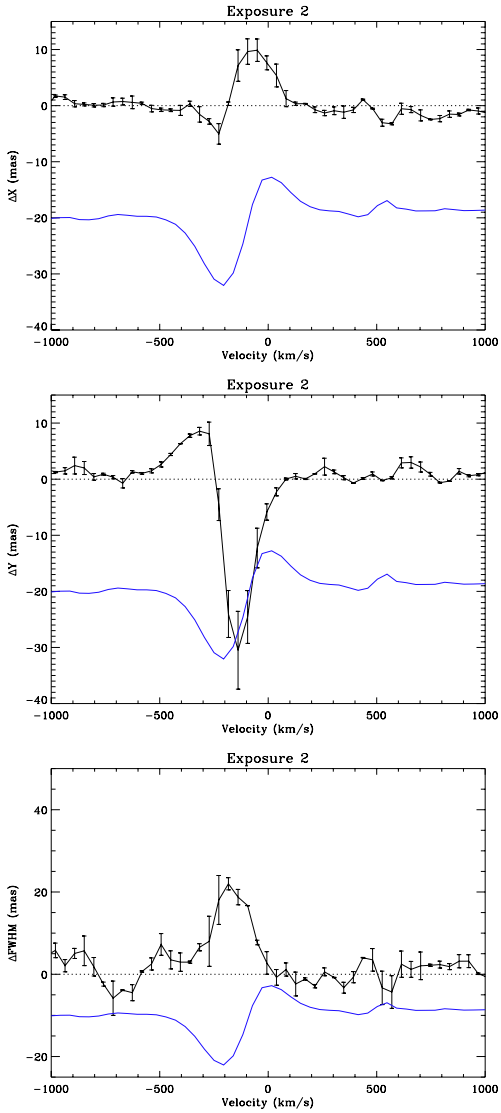

Fig. 2. Same as Fig. 1 for the second individual exposure taken.

ΔFWHM signals for the two exposures seem to have a different amplitude. However, the errors in the first exposure are high, and this is a $\lesssim 2\sigma$ effect.

We also looked for detection in the [OI]λ6300 Å line, but no [OI] emission is present in the spectrum. We derived an upper limit of detection of 21.4×10^{-19} Wm^{-2} Å^{-1} arcsec^{-2}, estimated as the three-sigma value in the spectrum placed at the continuum center. A spectro-astrometric study reveled no signature, as expected.

3.2. Test of the spectro-astrometric signal

The slit effect does not affect OASIS-like integral field spectrographs (Bacon et al. 1995). We thus analyzed the two main bias that can cause the observed spectro-astrometric signal: 1) flux contamination from the neighboring lenses during the extraction of the spectra and 2) a deficient wavelength calibration.

1) Flux contamination from neighboring lenses. As explained in Sect. 2, by default each spectra is extracted by summing in a five-pixel aperture. In the case of a contamination from neighboring lenses, the effect would be minimized and even eliminated by choosing a smaller aperture. However, after summing in a three-pixel aperture and in a one-pixel aperture, the observed effect remained. We therefore ruled this out as cause of the spectro-astrometric signal.

2) Deficient wavelength calibration. Model fitting between each spectrum in the field and the one at the stellar position was carried out. The spectra in each lens was modeled as a velocity-shifted and scaled version of the brightest lens spectra. This two-parameter model was fitted with a Levenberg-Marquardt algorithm. Only the points around the H_α profile (with $|v| < 10^3$ km s^{-1}) were considered in the fit. Top panels in Figs. 3 and 4 show the spatially distribution of the measured shift for each of the exposures taken. The continuum emission center corresponds to the position of the spectrum used as reference. A clear structure is seen in the center of the field with an approximate size of $\sim 2''$ in both spatial directions. We identify two clear distinct regions, one showing redshifted velocities up

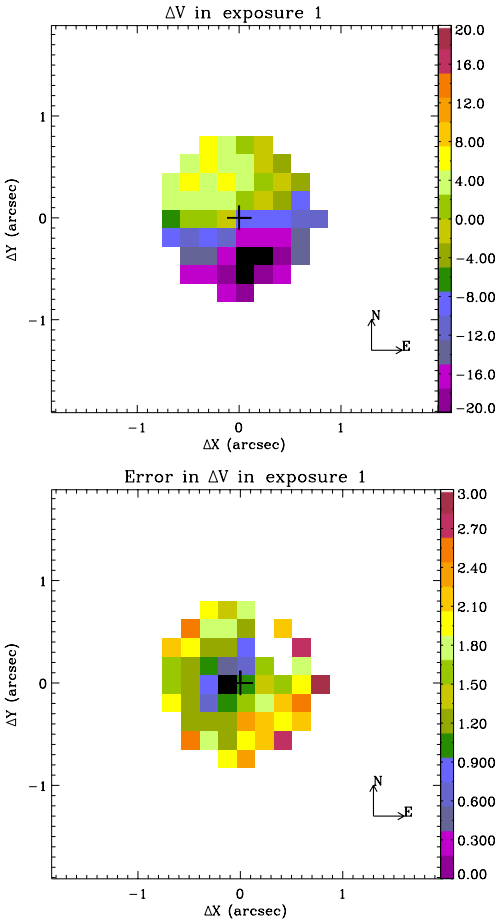

Fig. 3. *Top*: shift in velocity obtained from a cross-correlation of the P Cygni profile between the spectrum at the position of the star and each individual spectra in the field, for exposure 1. Color scale is km s^{-1}. The continuum emission center is marked as a black cross. The physical orientation is also given. *Bottom*: error in the shift also in km s^{-1}.

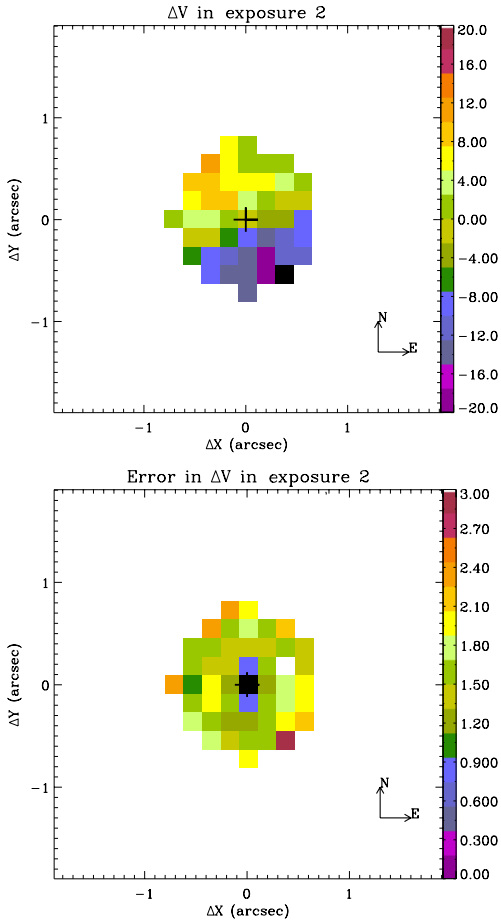

Fig. 4. Same as Fig. 3 for exposure 2.

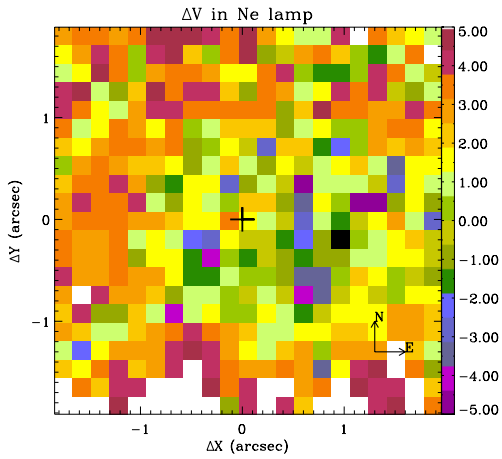

Fig. 5. Same as Fig. 3 but for the Neon arc used to wavelength calibration.

to ∼12 km s^{-1} in exposure 2, and the other blueshifted, almost symmetrical to the previous one, with values typically between –16 and –8 km s^{-1}. Bottom panels show the estimated errors for the velocities shift at each point. A quite well-defined imaginary line of PA ∼ 53 °separates the two regions of opposite velocities. An alternative check was made with a cross-correlation routine, CRSCOR in IDL, and the same results were found.

In the case of a problem in the wavelength calibration process we expect to find a similar structure in other images of the run, since the same procedure was used for all the cubes of the data set. We therefore applied the same study to the image of the neon arc used to carry out the wavelength calibration (Fig. 5). The arcs included five emission lines, which were fitted with Moffat functions with free amplitude and center, but with fixed shape (i.e., R and β (Moffat 1969)). The wavelength calibration correction for each lens was computed with a second-order polynomial. The velocity corrections for each lens, at H$_\alpha$, were compared with the brightest lens and no effect found. These results show that the effect is not due to a wavelength calibration bias.

4. Discussion and conclusion

We showed a clear spectro-astrometric signal observed in the H$_\alpha$ emission of the FUor star V1515 Cyg. The signal was tested for bias, and we concluded that the observed velocity structure observed in H$_\alpha$, shown in Figs. 3 and 4, is real, has a physical origin, and is characteristic of the H$_\alpha$ line, since no other emission is detected in other lines typically tracing outflows such as [OI]λ6300 Å, [NII]λ6584 Å, or [SII]$\lambda\lambda$6716, 6716. The velocity distribution of the observed structure suggests a rotating disk around the young star, which we can observe because of the scattering of the light by the disk. The FUor objects are assumed to be similar to T Tauri stars, consisting of a surrounding disk, maybe a remaining envelope, and an outflow. In fact, what we observe here is very similar to the observed velocity gradients in ^{12}CO images of protoplanetary disks with Keplerian rotation

in several T Tauri stars (e.g., Simon et al. 2000). In addition, several previous works on V1515 Cyg concluded that there is a need for an infalling envelope in order to fit the observed SED, in fitting the excess at 10 μm, and to explain the low K-band visibilities observed (Millan-Gabet et al. 2006; Green et al. 2006; Zhu et al. 2008). The models by Zhu et al. (2008) and by Green et al. (2006) also require the existence of an outflow cavity in the envelope. As shown by Kóspál (2011), this star is also surrounded by a nebula. As a result, the environmental medium in this star is a plausible option to produce scattering by dust either on the disk or on the envelope.

However, where is the light coming from? It may be stellar radiation scattered in a disk in Keplerian rotation, scattering by a dusty halo, or the light coming from an outflow. We briefly discuss these options on the basis of the results presented previously.

1) Disk in Keplerian rotation: as said before, the observed morphology of the structure strongly suggests scattering in a disk in Keplerian rotation. However, for the 1 kpc distance of this object and a typical velocity (V_k) of 10 km s^{-1} observed in Figs. 3 and 4 at a distance for the star of 1″(r), the expected central star mass, $M_* = V_k^2 \times r/G$, is ∼100 $M_\odot$ which is too high for this class of objects. Even in the regions where the observed velocity is ∼4 km s^{-1}, the derived star mass is ∼20 $M_\odot$, which is still too high. In the case of FU Ori a mass of 0.3 $M_\odot$ has been estimated by Zhu et al. (2007). Assuming a higher mass of ∼2 $M_\odot$, hence close to the highest masses observed in T Tauri stars (Calvet et al. 2004), the Keplerian velocity only explains ∼1 km s^{-1} of the observed values. An additional contribution is needed.

2) Dusty halo: the scattering light can also be produced by dusty halos, remnants of the original envelopes. Wheelwright et al. (2010) have carried out a spectro-astrometric study of several Herbig Ae/Be (HAe/Be) stars. They observe behavior in several of them similar of what has been observed here in V1515 Cyg. Large FWHM features occurred over absorption features in the emission profiles within small positional signatures (bottom and top panels of Figs. 1 and 2). They suggest that these signatures could trace extended structures that scatter the light, such as a disk/stellar wind (Azevedo et al. 2007), halos (Leinert et al. 2001; Monnier et al. 2006), or nebulosity. They considered the presence of dusty halos and carried out a simple model. In spite of the limits of their model, such as the unknown amount of light scattered and the extent of the halo, they reproduced the spectro-astrometric signatures observed for the PCygni profile observed over the H$_\alpha$ line in AB Aur quite well (their Fig. 4). In our case, however, the positional signature in the vertical direction is very different from the horizontal one and comparable to the FWHM features. This asymmetry could be caused by an outflow or by projection effects.

3) Outflow: Azevedo et al. (2007) show that the observed spectro-astrometric signal could also result from a wind. Some authors favor a nearly pole-on orientation of the system (Kenyon et al. 1991; Millan-Gabet et al. 2006; Zhu et al. 2008), in which case we would be seeing the outflow coming to us through the predicted cavity. The peak at ∼8–10 km s^{-1} (Figs. 3 and 4) could be caused by a shock in the outflow itself or against the envelope cavity on the disk or in the ambient medium. To explain the rest of the velocity structure, one simple explanation is that we are seeing the projected ΔV produced by rotation of an inner disk wind. Disk-wind models predict rotation of the outflow, and points on different sides of the jet with different velocities would be scattered by the disk or an envelope producing an observed ΔV. The projected ΔV of rotation from the outflow will be ∼10 km s^{-1}, which corresponds to the lower typical velocity differences measured by Coffey et al. (2007) in the case of DG Tau and interpreted as possible rotation signatures. However, for the regions with lower observed velocities, the derived velocities are too low for relating them with rotation signatures.

Unfortunately, this object is very faint, the signal-to-noise of our H$_\alpha$ line and the strong stellar continuum emission do not allow a more detailed analysis of this detection and for extracting more quantitative results and the disk parameters. In addition, the exact inclination of the system is unknown, so projection effects could play an important role in the interpretation.

In conclusion, the spatial distribution of the velocity structure observed in H$_\alpha$ suggests scattering by a disk or envelope surrounding the star. In that case, this would be one of the few spatial inferences of disks in FUor. Unfortunately our resolution does not allow a detailed parametrization of the emission observed in order to satisfactorily explain the velocity values observed. Observations at higher angular and spectral resolution are required. Since little is known about the exact structure of the disk and outflows in this class of objects, V1515 Cyg now appears to be an excellent candidate for future instruments with higher angular and spectral resolution.

Acknowledgements. This research was partially supported by FCT-Portugal through Project PTDC/CTE-AST/116561/2010. Vanessa Agra-Amboage also acknowledges financial and travel support through the Fundação para a Ciência e Tecnologia (FCT) under the contract SFRH/BPD/69670/2010. We thank Dr. Sylvie Cabrit and Dr. Catherine Dougados for their comments on the paper.

References

Audard, M., Ábrahám, P., Dunham, M. M., et al. 2014, in Protostars and Planets VI, eds. H. Beuther, R. Klessen, C. Dullemond, Th. Henning (University of Arizona Press) [arXiv:1401.3368]
Azevedo, R., Folha, D. F. M., Gameiro, J. F., & Calvet, N. 2007, ApJ, 670, 1234
Bacon, R., Adam, G., Baranne, A., et al. 1995, A&AS, 113, 347
Bastian, U., & Mundt, R. 1985, A&A, 144, 57
Benisty, M., Malbet, F., Dougados, C., et al. 2010, A&A, 517, L3
Calvet, N., Muzerolle, J., Briceño, C., et al. 2004, AJ, 128, 1294
Coffey, D., Bacciotti, F., Ray, T. P., Eislöffel, J., & Woitas, J. 2007, ApJ, 663, 350
Croswell, K., Hartmann, L., & Avrett, E. H. 1987, ApJ, 312, 227
Davies, B., Lumsden, S. L., Hoare, M. G., Oudmaijer, R. D., & de Wit, W.-J. 2010, MNRAS, 402, 1504
Green, J. D., Hartmann, L., Calvet, N., et al. 2006, ApJ, 648, 1099
Hartmann, L., & Kenyon, S. J. 1985, ApJ, 299, 462
Hartmann, L., & Kenyon, S. J. 1996, ARA&A, 34, 207
Herbig, G. H. 1977, ApJ, 217, 693
Herbig, G. H., Petrov, P. P., & Duemmler, R. 2003, ApJ, 595, 384
Horne, K. 1986, PASP, 98, 609
Kenyon, S. J., Hartmann, L. W., & Kolotilov, E. A. 1991, PASP, 103, 1069
Kóspál, Á. 2011, A&A, 535, A125
Leinert, C., Haas, M., Ábrahám, P., & Richichi, A. 2001, A&A, 375, 927
Millan-Gabet, R., Monnier, J. D., Akeson, R. L., et al. 2006, ApJ, 641, 547
Moffat, A. F. J. 1969, A&A, 3, 455
Monnier, J. D., Berger, J.-P., Millan-Gabet, R., et al. 2006, ApJ, 647, 444
Racine, R. 1968, AJ, 73, 233
Rodríguez, L. F., & Hartmann, L. W. 1992, Rev. Mex. Astron. Astrofis., 24, 135
Simon, M., Dutrey, A., & Guilloteau, S. 2000, ApJ, 545, 1034
Wheelwright, H. E., Oudmaijer, R. D., & Goodwin, S. P. 2010, MNRAS, 401, 1199
Whelan, E., & Garcia, P. 2008, in Jets from Young Stars II, eds. F. Bacciotti, L. Testi, & E. Whelan (Berlin: Springer Verlag), Lect. Notes Phys., 742 123
Whelan, E. T., Dougados, C., Perrin, M. D., et al. 2010, ApJ, 720, L119
Zhu, Z., Hartmann, L., Calvet, N., et al. 2007, ApJ, 669, 483
Zhu, Z., Hartmann, L., Calvet, N., et al. 2008, ApJ, 684, 1281